Measurement and comparison of complex impedance of silicon $p-i-n$ photodiodes at different temperatures

© H. Bayhan¶, S. Ozden

University of Muğla, Faculty of Art and Science, Department of Physics,
48000 Muğla, Turkey

(Получена 22 июня 2006 г. Принята к печати 30 августа 2006 г.)

The dark alternating current (ac), parameters of BPW34 and BPW41 (Vishay–Telefunken) silicon $p-i-n$ photodiodes are measured and compared at different temperatures using the impedance spectroscopy technique. The impedance plots are nearly semicircle and typically distorted on the high freguency side. For BPW41, the distortion apparently arises from one of the two interfaces as expected for a typical $p-i-n$ device. However, for BPW34, the presence of the distortion is attributed to the variation of photodiode capacitance and resistance with measurement frequency.

PACS: 85.60.Dw, 73.40.Lq

1. Introduction

Silicon based $p-i-n$ photodiodes coded as BPW34 and BPW41 have attracted much interest due to their wide range applications to industrial electronics, control and drive circuits etc. [1]. They are attractive because of their capability for high speed, high reliability, low power consumption and low production cost. Many investigations for commercial applications have been pursued, but some of the important electrical characteristics have not been revealed yet. The dynamic (dc) or the alternating current (ac) characteristics have received less attention, for which impedance spectroscopy can be used as a powerful analysis tool.

Impedance spectroscopy is a technique for the electrical characterisation of dielectrics by measuring the response of the material to an applied ac signal [2,3]. According to this technique, the complex impedance of a test sample, Z, which is expressed as $Z = Z' - jZ''$ where Z' is the real part and Z'' is the imaginary part, is measured directly in the frequency domain. A plot of Z' versus Z'' on complex plane for varying frequency gives the impedance spectrum of the test sample. From this, the equivalent circuit parameters which are representative of the physical processes taking place in the sample, can be determined.

In this study, we investigate the ac parameters of commercial BPW34 and BWP41 (Vishay–Telefunken) $p-i-n$ photodiodes by varying the measurement temperature from 250 to 295 K at 0.5 V bias voltage. Frequency dependent impedance data are obtained in the range from 10 Hz to 10 MHz.

2. Experimental

The dark ac impedance data of $p-i-n$ devices are measured using Hewlett Packard HP 4192A impedance analyser in the frequency range from 10 Hz to 10 MHz. Since the typical $p-i-n$ device is a non-linear device, the amplitude of the applied signal should be less than thermal voltage ($V_T \approx 26$ mV at 22°C). The ac signal of amplitude 10 mV is selected to ensure that the response of the system is linear piece-wise to good approximation. The shield cables are used for the connections to reduce noise from the environment. The typical photodiode is mounted in the sample holder of the helium cryostat (Oxford) and all measurements are performed in vacuum. The temperature of the sampe holder is varied from 250 to 300 K with steps of 15 K and value of the bias voltage was selected as 0.5 V.

3. Results and discussions

Nyquist plots of the BPW34 and BPW41 photodiodes at different temperatures varying from 250 to 295 K are shown in Figs. 1, *a* and *b*, respectively. It can be observed that the resistance of BPW41 are approximately twice that of BPW34 at the same temperatures. All impedance plots are very close to semicircle at low frequencies and they show some distortion at high frequencies.

It can be observed from Figs. 2, *a* and *b* that an equivalent circuit represented by a parallel resistor R_p, and capacitor C_0 network connected with a series resistance R_s accurately fits to the high frequency data of both photodiodes. The R_s and R_p values are estimated as 115 and 340 Ω for BPW34 and 1900 and 5100 Ω for BPW41, respectively. The value of C_0, which is the geometric capacitance measured at 1 MHz frequency and at zero dc voltage (82 pF for BPW34; 73 pF for BPW41) is used for the fitting procedure.

In practice, the equivalent circuit of a typical $p-i-n$ structure can be represented by two RC sub-circuits (parallel resistors R_{p1}, R_{p2} and capacitors C_{01}, C_{02}) in series with

¶ E-mail: hbayhan@mu.edu.tr

a resistor R_s as show below,

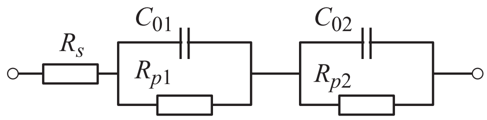

R_s is proposed to be almost entirely created by the bulk layers and ohmic contacts. R_{p1}, C_{01} and R_{p2}, C_{02} are resistances and capacitances which corresponds to n/i and i/p interfaces in the $p{-}i{-}n$ structire [2]. However, Bode plots given in Figs 3, a and b clearly reveal that only the complex impedance plots of BPW41 have multiple time constants. The phase angle $\theta = \mathrm{tg}^{-1}(Z''/Z')$vs lg$f$ plots of BPW34 yield a single peak which varies from 10 to ~ 20 kHz as the temperature varies from 295 to 285 K (Fig. 3, a).

All these may possibly suggest that both space charge regions, namely n/i and i/p interfaces, could have important role for the ac response of the BPW41. However for BPW34, either p/i or i/n interface could play a more relevant role for the ac conduction in the temperature region under consideration. Although we do not know the definite energy band structure and the doping profiles of different layers in these devices, it is generally accepted that the i-region in the $p{-}i{-}n$ photodiodes is slightly of n-type. If we assume that the n/i junction is nearly ohmic, we can reasonably infer that the electrical characterictics of BPW34 are mainly determined by the i/p interface.

Figs. 1, a and 2, a indicated that the semicircular nature of the impedance plots at high frequencies tend to a straight line with a slope of around 65°. A possible physical origin for this deviation could be related to variation of device capacitance and resistance of BPW34 with the measurement frequency similarly as reported for $p{-}n$ junction solar cells in the literature [4–7]. It is generally assumed that the electrical analogue circuit of a solar cell can be described by a single RC network connected with a series resistance R_s. The RC network is composed of two types of capacitances (i. e. diffusion and transition (or depletion region) capacitances, C_d and C_T) and resistances (i. e. diffusion and transition resistances, R_d and R_T) which are all connected parallel each with other [4,8]. C_d and R_d are due to the gradient of the charge density inside the device and the bulk resistance of the space charge region, respectively. R_T is the resistance due to recombination of

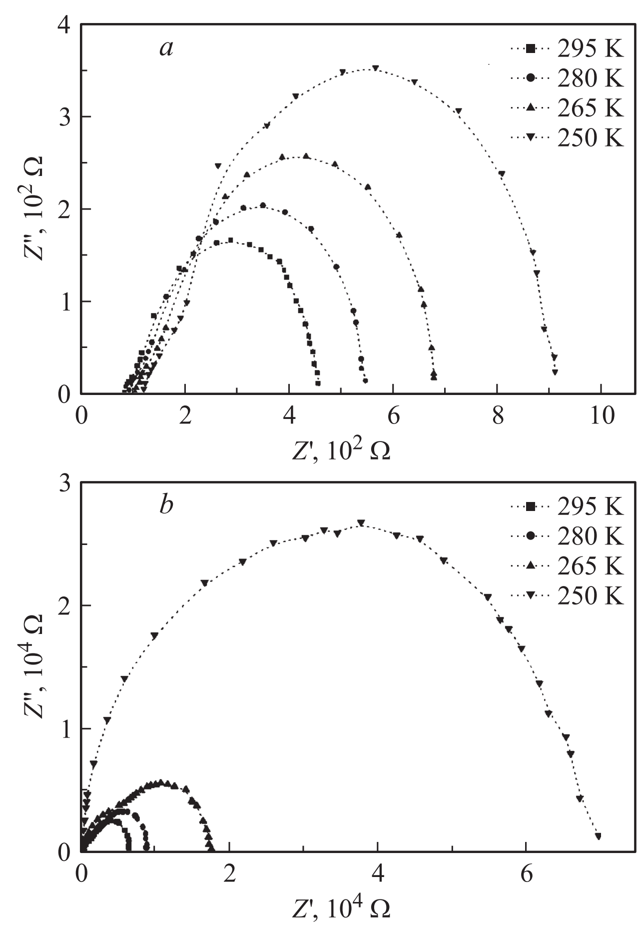

Figure 1. Nyquist plots of BWP34 (a) and BWP41 (b) photodiodes at different temperatures. The dotted lines are present to guide the eye.

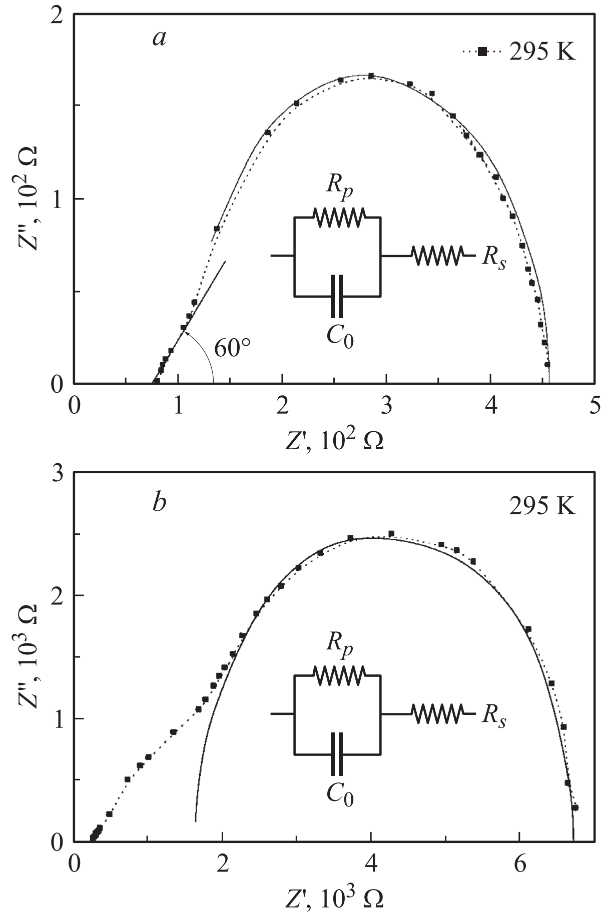

Figure 2. Experimental (dots) and calculated (solid line) complex impedance data with the corresponding RC equivalent circuit for BWP34 (a) and BWP41 (b) photodiodes at the temperature 295 K.

free carriers in the space charge region and C_T is the space charge leyer capacitance.

The temperature dependent values for R_s and the equivalent of parallel resistance combination $(R_d \parallel R_T)$ for BPW34 are estimated from the low and high frequency intercepts of the semicircular variations on the axis of Fig. 1, *a*. The value $R_d \parallel R_T$ decreases with temperature because of the photodiode current increase with temperature. The $C_T + C_d$ sum values at different tempertures are estimated by using the value f which is almost constant at ~ 5 kHz around maximum $Z''_{\max}$ [4],

$$Z''_{\max} = \frac{1}{2\pi f (C_T + C_d)}$$

All evaluated parameters are done in the Table.

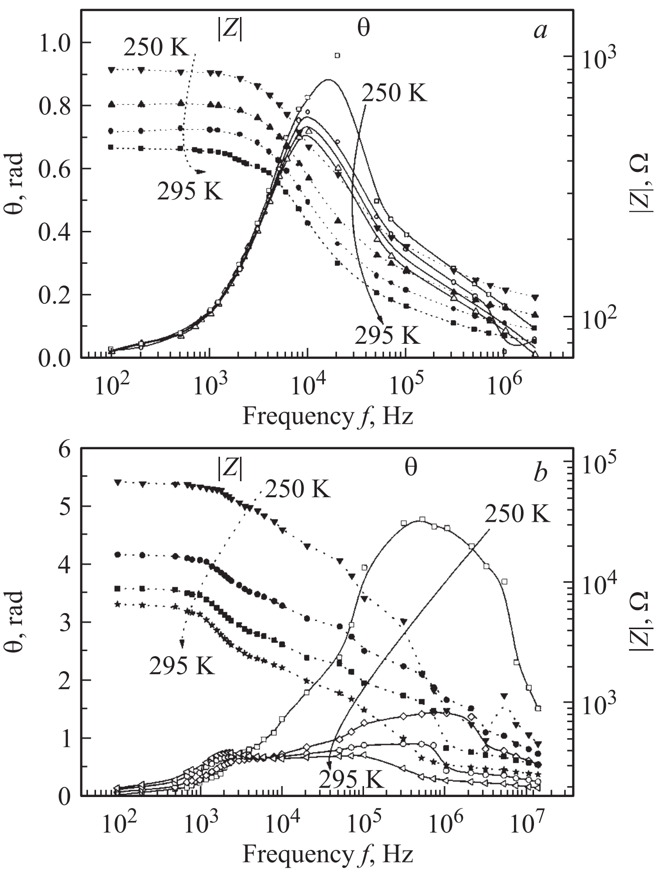

Figure 3. Bode plots for BWP34 (*a*) and BWP41 (*b*) at different temperatures. The solid symbols correspond to the data for absolute magnitude of the impedance $|Z| = \sqrt{Z'^2 + Z''^2}$ and the open symbols correspond to the data for the phase angle θ which is defined by $\mathrm{tg}\,\theta = Z''/Z'$. The dot and solid lines are present to guide the eye.

Variation of R_T, $C_T + C_d$ and $R_d \parallel R_T$ with temperature for BPW34

T, K	R_s, Ω	$C_T + C_d$, nF	$R_d \parallel R_T$, Ω
250	184	192	723
265	152	155	515
280	133	123	412
295	100	89	355

For further analysis of the photodiode capacitance origin at different temperatures, $\lg(C_T + C_d)$ is plotted as a function of $1/T$ in Fig. 4. It is observed that $(C_T + C_d)$ is exponentially related to the measurement temperature. Since the value of depletion region capacitance C_T is expected to be almost the same at different temperatures [7], the exponential variation could be mainly due to the contribution of diffusion capacitance [4,9].

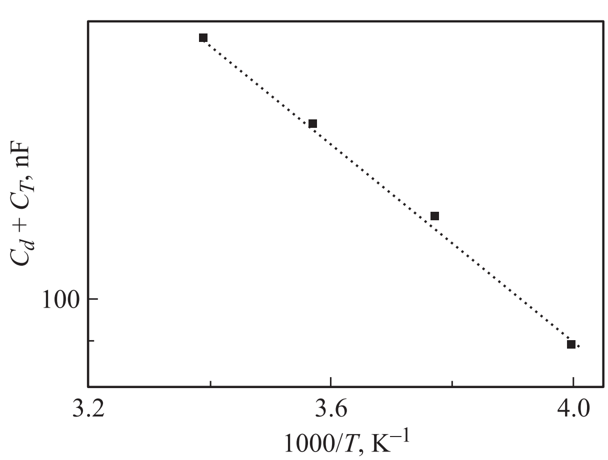

Figure 4. The variation of the equivalent photodiode capacitance $C_T + C_d$, as a function of temperature for BPW34. The dotted line is present to guide the eye.

4. Conclusions

The ac impedances of commercially available BPW34 and BPW41 silicon $p-i-n$ photodiodes are studied and compared for different measurement temperatures from 250 to 295 K. The impedance spectra of both photodiodes are characterised by nearly semicircular shape apparently having some distortion in the high frequency region. The Bode plots of BPW41 have revealed that this distortion could be related to a second *RC* network added to one of the juction. This may be attributed to the effective role of both interfaces, i. e. n/i and i/p, to the ac response of the photodiodes.

For BPW34, the predominance of a single time constant could possibly be correlated to the single sided juction operation. The linearly shaped distortion observed on the high frequency region of the impedance plots can be attributed to variation of the photodiode equivalent capacitance and the resistance with the measurement frequency.

References

[1] Vishay Telefunken. *Data sheets of BPW34 and BPW41 photodiodes.* http://www.vishay.com/photodetectors (accessed May 2006).

[2] J.R. Macdonald. *Impedance Spectroscopy* (John Wiley and Sons, N.Y., 1987).
[3] E. Barsoukov, J.R. Macdonald. *Impedance Spectroscopy: Theory, Experiment and Applications*, 2nd edition (John Wiley and Sons Inc, Habokem, N.Y., 2005).
[4] M.S. Suresh. Sol. Energy Mater. and Solar Cells, **43**, 21 (1996).
[5] R.A. Kumar, M.S. Suresh, J. Nagaraju. Sol. Energy Mater. and Solar Cells, **60**, 155 (2000).
[6] R.A. Kumar, M.S. Suresh. Rev. Sci. Instrum., **72**, 3422 (2001).
[7] R.A. Kumar, M.S. Suresh, J. Nagaraju. Sol. Energy Mater. and Solar Cells, **85**, 397 (2005).
[8] H.S. Rauschenbach. *Solar Array Design Hand Book* (Van Nosrtrand Reinhold, N.Y., 1980).
[9] J. Millman, C.C. Halkias. *Integrated Electronics* (Mc Graw-Hill, N.Y., 1972).

Редактор Л.В. Шаронова